

Tracing the source of the different magnetic behavior in the two phases of the bistable $(\text{BDTA})_2[\text{Co}(\text{mnt})_2]$ compound

Sergi Vela, Mercè Deumal*, Jordi Ribas-Arino*, Juan J. Novoa

Departament de Química Física & IQTCUB, Facultat de Química, Universitat de Barcelona.
Martí i Franquès 1, Barcelona, Spain

ABSTRACT: A complete computational study of the magnetic properties of the two known phases of the bistable $(\text{BDTA})_2[\text{Co}(\text{mnt})_2]$ compound is presented. The origin of their different magnetic properties can be traced to a variation in the values of the g -tensor, together with a hitherto unknown change in the J_{AB} values and their magnetic topology.

In the quest for new technologies suitable for future memory and switching devices, molecular materials that can be switched between two states by the application of an external stimulus (e.g. heat, pressure) have attracted much attention.^{1,2,3} For these bistable materials to be of technological interest, the phase transitions between the two polymorphs must be abrupt, besides presenting a hysteresis loop.^{3,4} Despite the plethora of materials exhibiting these properties,^{5,6,7,8} a rational design of new molecule-based bistable materials is not yet fully attainable, since there is no proper knowledge of the mechanism responsible for this behavior at the microscopic level.⁹

$(\text{BDTA})_2[\text{Co}(\text{mnt})_2]$, **1**, is a remarkable bistable system reported by Awaga and coworkers,^{10,11} whose two polymorphic phases present different magnetic properties (BDTA = 1,3,2-benzodithiazolyl; mnt^{2-} = maleonitriledithiolate). Each neutral $(\text{BDTA})_2[\text{Co}(\text{mnt})_2]$ unit presents a doublet ground state (its geometry, SOMOs and spin densities for both phases can be found in the Supporting Information). The different magnetic properties of the two phases of **1** were originally explained solely in terms of a change in the g -tensor value upon the phase transition. This is in contrast with other bistable systems where the variation in the magnetic properties was traced to changes in the values of the microscopic exchange interactions, J_{AB} , in going from one phase to the other one.¹² Such a different interpretation prompted us to carry out a theoretical First-Principles Bottom-Up (FPBU)¹³ study where the shape of the magnetic susceptibility curves of the two phases of **1** was investigated over the whole range of experimentally measured temperatures (0-300K). Based on this study, we have been able to provide a sound explanation for the different magnetic properties of the two phases of **1**.

As observed in Fig. 1a, $(\text{BDTA})_2[\text{Co}(\text{mnt})_2]$ exhibits an abrupt jump in the experimental χT (χ = molar magnetic susceptibility) at ca. 190 K with a hysteresis width of 20 K.¹⁰ Such transition, in addition to changes in crystal symmetry and packing, is accompanied by the formation/cleavage of an axially coordinated $\text{Co}\cdots\text{S}$ bond, involving one sulfur atom of BDTA. The origin of such jump in χT has been previously attributed¹⁰ to a change in the g -tensor of **1** (from 2.55 at high

temperature (HT) to 2.29 at low temperature (LT)) due to a charge transfer process that takes place when this $\text{Co}\cdots\text{S}$ bond is formed/broken.¹⁰ Theoretical calculations have confirmed such metal-to-ligand charge transfer.¹⁴ Although it is well known^{12,15} that the size of the magnetic exchange J_{AB} interactions and their magnetic topology (the network of connectivity that the non-negligible J_{AB} interactions build within the crystal) are essential in defining the macroscopic magnetic properties, the changes in J_{AB} 's and their topology upon the phase transition surprisingly have not yet been addressed. The reason might be twofold: (i) a lack of good models to fit the experimental $\chi T(T)$ data for bulk magnetic systems, and (ii) the shape of the χT curve in the HT phase, which hints at the existence of very small J_{AB} values. One should thus wonder about the impact of the J_{AB} 's and their topology on the computed χT curves for the HT and LT polymorphs of **1** and, particularly, on the shape of the hysteresis cycle.

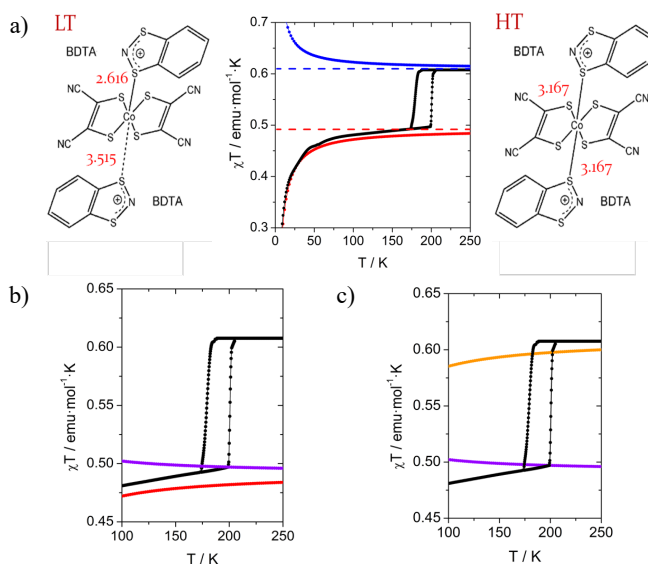


Figure 1: Comparison between the experimental (black) and computed χ curves: a) Using the computed J_{AB} values and the experimental g -tensors for each phase (HT- g^{HT} and LT- g^{LT} curves in blue and red; dashed lines correspond to χT values obtained for both phases when all J_{AB} interactions are set to zero corresponding to the Curie law regime); b) Keeping the computed J_{AB} values but forcing the g -tensor for both phases to be equal to that for LT (HT- g^{LT} and LT- g^{LT} curves in purple and red); c) Keeping the g -tensor but exchanging magnetic topology between HT and LT phases (HT- g^{LT} and LT- g^{HT} in purple and orange). The geometries of $(\text{BDTA})_2[\text{Co}(\text{mnt})_2]$ units in the LT and HT phases are displayed in (a).

Table 1. Magnetic exchange coupling J_{AB} (in cm^{-1}) for LT and HT phases of **1, computed with (i) a basis set of TZV quality and (ii) def2-tzvp basis set (in parenthesis). Also given are the corresponding Co \cdots Co distances (in \AA).**

LT		HT	
d(Co \cdots Co)	J_{AB}	d(Co \cdots Co)	J_{AB}
6.792	-3.3 (-3.6)	7.017	0.3 (0.3)
7.212	-0.5	7.275	1.5 (1.9)
8.605	-0.2		
8.391	-2.4		
9.313	0.2		

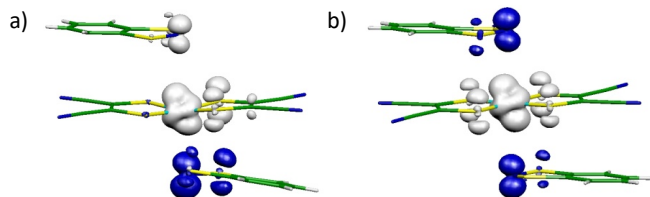


Figure 2. Spin densities of the (BDTA) $_2$ [Co(mnt) $_2$] complex for the (a) LT and (b) HT phases. Notice the different sign of the upper BDTA unit in both phases.

The J_{AB} interactions for all unique radical-pairs present in the HT and LT crystal structures of **1** and, based on them, the χ T curves, have been evaluated using our FPBU work strategy.¹³ For the LT polymorph characterized at 100 K, five unique 1 \cdots 1 radical pairs were found to present a non-negligible¹⁶ J_{AB} value (their Co \cdots Co distances ranging from 6.72 to 9.31 \AA , see Table 1 and Supporting Information). Analogously, two non-negligible 1 \cdots 1 radical pairs were found in the HT polymorph characterized at 253 K. Using these J_{AB} values and the magnetic topologies that they define (see below), one can compute the χ T curves with the experimental values¹⁰ for the g-tensor: $g^{\text{LT}}=2.29$ for LT, $g^{\text{HT}}=2.55$ for HT (Fig. 1a).¹⁷ Note that the computed χ T curves properly reproduce not only the experimental curves for the LT and HT polymorphs *over the whole range of temperatures*, but also the gap between them. Also note that while the χ^{LT} curve is dominated by AFM interactions, the χ^{HT} curve is dominated by FM interactions, consistently with the results collected in Table 1. Such important change in the sign of the magnetic interaction can be attributed not only to geometrical changes but also to noticeable differences in the topology of the spin density of the (BDTA) $_2$ [Co(mnt) $_2$] units in both phases (see Fig. 2 and Supporting Information for further discussion on spin density and SOMOs). There is no experimental data to confirm the dominant FM nature of the HT phase at low temperature. Calculations with the larger def2-tzvp¹⁸ basis set on selected dimers of the HT and LT phases confirm the accuracy of the computed J_{AB} values and their topologies (see Supporting Information for details). Previous experience on other FM systems indicates that the FPBU computational methodology provides an appropriate description of the J_{AB} microscopic parameters and the macroscopic properties in the region of temperatures for the HT/LT phase transition.¹⁵

One can now analyze the relative importance of the g-tensor on the $\chi^{\text{HT}} - \chi^{\text{LT}}$ jump present in **1** (Fig. 1). This can be evaluated by comparing the previously computed $\chi^{\text{HT}}-g^{\text{HT}}$ and $\chi^{\text{LT}}-g^{\text{LT}}$ curves (Fig. 1a) with those obtained using the

same g-tensor (e.g. $g^{\text{LT}}=2.29$) for both phases (see Fig. 1b). A comparison of the χ^{HT} curves in Figures 1a (blue) and 1b (purple) shows that the latter curve is significantly shifted downward in the whole temperature range. The $[\chi^{\text{HT}}-g^{\text{LT}}] - [\chi^{\text{LT}}-g^{\text{LT}}]$ jump in Fig. 1b at *ca.* 190 K, whose origin is exclusively due to the J_{AB} interactions, is around a non-negligible 16% of the experimental jump at the same temperature. Besides, Fig. 1c clearly shows that the magnetic topology plays a key role in tuning the slope of the χ T curves within the hysteresis loop, i.e. if one uses the wrong magnetic topology with the correct g-factor in the LT ($\chi^{\text{HT}}-g^{\text{LT}}$) phase (and vice versa), the slope of the resulting χ T curve has opposite sign compared to experiment. All these results prove that both changes in the g-factor and magnetic topology are indeed at the origin of the hysteresis behavior.

The different magnetic susceptibility of the HT and LT phases can be better understood by inspecting in detail their magnetic topologies (see Fig. 3 and Supporting Information). Each phase can be visualized as the repetition of a magnetic building block along the symmetry elements of the crystal. The magnetic building block for the HT phase has rhomboidal shape, with FM exchange couplings in the long and short edges (Table 1). This pattern gives rise to 2D planes, consisting of a set of weakly interacting (+0.3 cm^{-1}) FM chains (+1.5 cm^{-1}) (Fig. 3a). These 2D planes stack in the third dimension, although remaining magnetically isolated (Fig. 3b). The rhomboidal shape of the magnetic building block observed in HT is basically preserved in the LT phase (Table 1), but with relevant modifications. First of all, the 2D planes in LT are corrugated and can now be seen as a set of alternating 1D AFM chains (-3.3 and -2.4 cm^{-1}) that weakly interact among them (Fig. 3c). The planes stack along the third direction and the resulting overall magnetic topology is, once again, a pile of magnetically isolated 2D planes (Fig. 3d). Therefore, the analysis of these two magnetic topologies clearly explains why the χ^{LT} curve is dominated by AFM interactions, whereas χ^{HT} presents dominant FM interactions (see Fig. 1), and allows to associate these dominant interactions with specific radical-pairs.

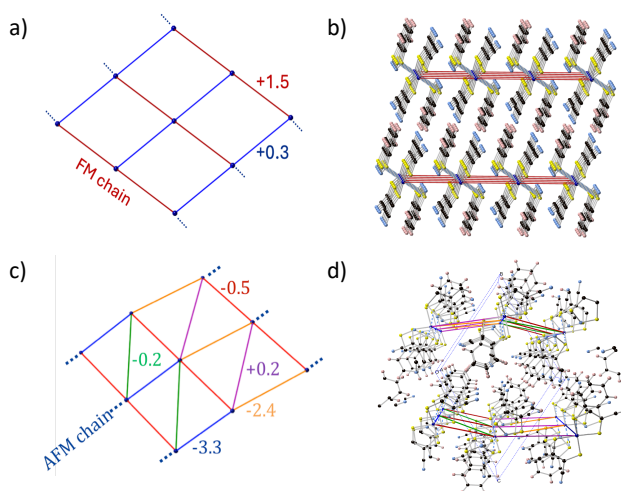


Figure 3. Magnetic topology for the (a-b) HT and (c-d) LT phases. The colored lines represent J_{AB} (in cm^{-1}) between radicals (blue dots). (a,c). Isolated 2D magnetic layers. (b,d) View of the magnetic topology within the crystal packing consisting in magnetically isolated 2D planes

In summary, by doing a First-principles Bottom-up study¹³ of the magnetic interactions in the LT and HT phases of (BDTA)₂[Co(mnt)₂], we have gained a full understanding of the change in magnetic properties upon phase transition of the bistable compound **1**. Using the computed J_{AB} values and their topology we have reproduced and rationalized the experimental χT curves in the whole range of measured temperatures, including the hysteresis loop present in the bistability region. Our calculations allow to trace the origin of the jump in the HT and LT χT curves mainly to the variation in the g-tensor, in good agreement with previous approximations.¹⁰ Yet the role of the J_{AB} interactions must not be neglected. In fact, the dominant AFM behavior of the experimental χT^{LT} curve at low temperatures can only be reproduced once the J_{AB} values are also taken into consideration. For the χT^{HT} curve, our study uncovers a dominant FM behavior. This low temperature change from a dominant FM (HT phase) to a dominant AFM (LT phase) behavior, suggests the possibility of new photo-magnetic studies. Overall, this work constitutes another example of how theoretical calculations can provide a most valuable insight to interpret, rationalize and predict magnetic properties of molecule-based materials.

COMPUTATIONAL DETAILS

Based on the First-principles Bottom-up work strategy,¹³ all symmetry unique radical-radical 1...1 exchange couplings (J_{AB}) were calculated for dimers extracted from the crystal structure (selected by considering a cutoff distance of 10 Å between Co atoms; see Supporting Information for the dimer geometries). The radicals here are doublets ($S=1/2$). For the following Heisenberg Hamiltonian, $\hat{H}_{AB} = -J_{AB} \hat{S}_A \cdot \hat{S}_B$, the value of J_{AB} for each AB pair is computed as the energy difference between the pair open-shell singlet S and triplet T states, $\Delta E^{S-T} = 2(E^{BS} - E^T) = 2J_{AB}$ (note that the Broken Symmetry BS approach¹⁹ was used to properly describe the open-shell singlet state). The magnetic models employed to compute the χT curves are displayed in the Supporting Information. Energy evaluations were first done using the B3LYP²⁰ functional, as implemented in Gaussian03²¹, with TZV basis set²² for Co atoms, and 6-31+G* basis set²³ for the remaining atoms. The numerical error associated with the corresponding final individual energies is 10^{-7} au. It follows that the evaluation of J_{AB} implies a numerical error of 0.04 cm^{-1} .

The g-tensor calculations were done using the SOMF(1X) approximation²⁵ implemented in the ORCA2.7 package,²⁵ employing the PBE0²⁶ functional and the def2-tzvp¹⁸ basis set. Calculations with other basis sets indicate that this property is non-basis set dependent, as suggested in the literature.²⁵

Supporting Information. Details on the electronic structures of (BDTA)₂[Co(mnt)₂] radical. Assessment of the accuracy in J_{AB} calculation. Selected magnetic models for χT simulation. This material is available free of charge via the Internet at <http://pubs.acs.org>.

CORRESPONDING AUTHORS

* j.ribas@ub.edu, merce.deumal@ub.edu

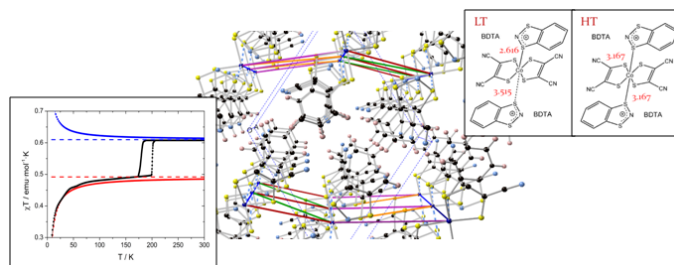
ACKNOWLEDGMENT

We thank the Spanish Government for support (projects MAT2008-02032 and MAT2011-25972), a Ph.D. grant to S.V., and a "Ramón y Cajal" fellowship to J.R-A. We also thank the Catalan DURSI (2009-SGR-1203) and the computer time allocated by CESCA and BSC.

REFERENCES

- (1) Balzani, V.; Credi, A.; Venturi, M. *Molecular Devices and Machines. A Journey into the Nanoworld*, Wiley-VCH, **2003**.
- (2) Kahn, O.; Martínez, C.J. *Science*. **1998**, *279*, 44.
- (3) Létard, J-F.; Guionneau, P.; Goux-Capes, L. *Top. Curr. Chem.* **2004**, *235*, 221.
- (4) Kahn, O.; Launay, J.P. *Chemtronics*, **1988**, *3*, 140.
- (5) Sato, O.; Tao, J.; Zhang, Y-Z. *Angew. Chem. Int. Ed.* **2007**, *46*, 2152.
- (6) Transition-metal spin-crossover complexes: (a) Gütllich, P.; Goodwin, H.A. *Top. Curr. Chem.* **2004**, *233*, 1; (b) Gamez, P.; Costa, J.S.; Quesada, M.; Aromí, G. *Dalton Trans.* **2009**, 7845; (c) Halcrow, M.A. *Chem. Soc. Rev.* **2011**, *40*, 4119.
- (7) Purely organic radical compounds: (a) Fujita, W.; Awaga, K. *Science*, **1999**, *286*, 261. (b) Itkis, M.E.; Chi, X.; Cordes, A.W.; Haddon, R.C. *Science* **2002**, *296*, 1443. (c) Hicks, R.G. *Nat. Chem.* **2011**, *3*, 189.
- (8) Charge-transfer complexes: (a) Hendrickson, D.N.; Pierpoint, C.G. *Top. Curr. Chem.* **2004**, *234*, 63; (b) Berlinguette, C.P.; Dragulescu-Andrasi, A.; Sieber, A.; Galan-Mascaros, J.R.; Güdel, H.-U.; Achim, C.; Dunbar, K.R. *J. Am. Chem. Soc.* **2004**, *126*, 6222; (c) Sessoli, R. *Nat. Chem.* **2010**, *2*, 346.
- (9) Real, J.A.; Gaspar, A.B.; Niel, V.; Muñoz, M.C. *Coord. Chem. Rev.* **2003**, *236*, 121.
- (10) Umezono, Y.; Fujita, W.; Awaga, K. *J. Am. Chem. Soc.* **2006**, *128*, 1084.
- (11) Fujita, W.; Awaga, K.; Nakazawa, Y.; Saito, K.; Sorai, M. *Chem. Phys. Lett.* **2002**, *352*, 348.
- (12) See, for instance: (a) Clarke, C.S.; Jornet-Somoza, J.; Mota, F.; Novoa, J.J.; Deumal, M. *J. Am. Chem. Soc.* **2010**, *132*, 17817; (b) Rawson, J.M.; Alberola, A.; Whalley, A.; *J. Mater. Chem.*, **2006**, *16*, 2560; (c) Lekin, K.; Winter, S.M.; Downey, L.E.; Bao, X.; Tse, J.S.; Desgreniers, S.; Secco, R.A.; Dube, P.A.; Oakley, R.T. *J. Am. Chem. Soc.*, **2010**, *132*, 16212.
- (13) Deumal, M.; Bearpark, M.J.; Novoa, J.J.; Robb, M.A. *J. Phys. Chem. A* **2002**, *106*, 1299.
- (14) Kepenekian, M.; Le Guennic, B.; Awaga, K.; Robert, V. *Phys. Chem. Chem. Phys.* **2009**, *11*, 6066.
- (15) Novoa, J.J.; Deumal, M.; Jornet-Somoza, J. *Chem. Soc. Rev.* **2011**, *40*, 3182; Norel, L.; Rota, J-B.; Chamoreau, L-M.; Pilet, G.; Robert, V.; Train, C. *Angew. Chem.* **2011**, *123*, 7266; Vérot, M. Bréfuel, N.; Pécaut, J.; Train, C.; Robert, V. *Chem. Asian J.* **2012**, *7*, 380.
- (16) In practice, J_{AB} 's whose absolute value is larger than 0.05 cm^{-1} .
- (17) Our computed g-tensor values on a (BDTA)₂[Co(mnt)₂] moiety are $g^{\text{LT}}=2.18$ and $g^{\text{HT}}=2.22$ to be compared to experimental $g^{\text{LT}}=2.29 \pm 0.10$ and $g^{\text{HT}}=2.55 \pm 0.10$ data.¹⁰ Thus, we have opted for the combined use of experimental data together with computed J_{AB} values, which has already been proven to be a successful strategy. See 15a and Petit, S.; Borshch, S.A.; Robert, V. *J. Am. Chem. Soc.* **2003**, *125*, 3959.
- (18) Weigend, F.; Ahlrichs, R. *Phys. Chem. Chem. Phys.*, **2005**, *7*, 3297-3305.
- (19) (a) Noodleman, L. *J. Chem. Phys.* **1981**, *74*, 5737. (b) Noodleman, L.; Davidson, E. R. *Chem. Phys.* **1986**, *109*, 131.
- (20) Becke, A.D. *J. Chem. Phys.* **1996**, *104*, 1040.
- (21) Gaussian 03, Revision C.02, M. J. Frisch et al., Gaussian, Inc., Wallingford CT, **2004**.
- (22) Schaefer, A.; Huber, C.; Ahlrichs, R. *J. Chem. Phys.*, **1994**, *100*, 5829.
- (23) Ditchfield, R.; Hehre, W.J.; Pople, J.A. *J. Chem. Phys.*, **1971**, *54*, 724
- (24) (a) Neese, F. *J. Chem. Phys.* **2005**, *122*, 034107. (b) Neese, F. *J. Chem. Phys.* **2001**, *115*, 11080.
- (25) Adamo, C.; Barone, V. *J. Chem. Phys.*, **1999**, *110*, 6158.

Table of Contents - Graphic



Based on a theoretical First-Principles Bottom-Up approach, we have gained a full understanding of the change in magnetic properties upon phase transition of the bistable $(\text{BDTA})_2[\text{Co}(\text{mnt})_2]$ compound. The origin of the abrupt jump in the magnetic susceptibility χT curve can be traced to a variation in the values of the g -tensor, together with a hitherto unknown change in the J_{AB} values and their magnetic topology.